HHS Public Access

Author manuscript

J Thorac Oncol. Author manuscript; available in PMC 2019 December 01.

Published in final edited form as:

J Thorac Oncol. 2018 December ; 13(12): 1884–1896. doi:10.1016/j.jtho.2018.09.012.

Immune marker profiling and PD-L1 expression across Non-Small Cell Lung Cancer mutations

Maria I. Toki[1], **Nikita Mani**[1], **James W. Smithy**[1], **Yuting Liu**[1], **Mehmet Altan**[2], **Brad Wasserman**[1], **Rasikh Tuktamyshov**[3], **Kurt Schalper**[1,3], **Konstantinos N. Syrigos**[4], and **David L. Rimm**[1,3]

[1]Department of Pathology, Yale University School of Medicine, New Haven, CT, USA

[2]Department of Thoracic/Head &Neck Medical Oncology, The University of Texas MD Anderson Cancer Center, Houston, TX, USA

[3]Department of Medicine, Yale University School of Medicine, New Haven, CT, USA

[4]3rd Department of Medicine, University of Athens, School of Medicine, Sotiria General Hospital, Athens, Greece

Abstract

Purpose: PD-1/PD-L1 axis inhibitors have been proven effective, especially in patients with tumors expressing Programmed Death Ligand 1 (PD-L1). Their clinical efficacy in patients with epidermal growth factor receptor (EGFR) activating mutations is still unclear, while KRAS mutations seem to be associated with good response.

Experimental Design: We used multiplexed quantitative immunofluorescence (QIF) to investigate PD-L1 expression and to characterize Tumor Infiltrating Lymphocyte (TIL) populations and their activation status in over 150 Non-Small Cell Lung Cancer (NSCLC) patients with known mutation status.

Results: PD-L1 expression was significantly lower in EGFR mutant compared to KRAS mutant and EGFR/KRAS Wild Type (WT) tumors. KRAS mutant tumors were more inflamed with higher CD4+, CD8+ and CD20+ TILs. Subgroup analysis by TILs activation status revealed that EGFR mutants had a high frequency of inactive TILs even though lymphocytes were present in the tumor microenvironment. In contrast, in KRAS mutants, when TILs were present, they were almost always active. Additionally, we found differences between EGFR mutation sites in CD8+ expression and TILs activation profile. Finally, activated EGFR correlated with increased PD-L1

*Corresponding Author: Maria I. Toki MD, MSc, Dept. of Pathology, BML 116, Yale University School of Medicine, 310 Cedar St. PO Box 208023, New Haven, CT 06520-8023, Phone: 203-737-4205, FAX: 203-737-5089, maria.toki@yale.edu.

Conflict of Interest: Dr. Rimm declares that in the last two years he has served as a consultant to Astra Zeneca, Agendia, Bethyl Labs, Biocept, BMS, Cell Signaling Technology, Cernostics, ClearSight, FivePrime, Genoptix/Novartis, Metamark Genetics, Merck, OptraScan, Perkin Elmer, and Ultivue. Dr. Schalper reports personal fees from Celgene, Moderna and Shattuck Labs, grants from Vasculox (Tioma), Takeda, Tesaro, Moderna, Surface Oncology, Pierre-Fabre, Merck, BMS, Navigate Biopharma, outside the submitted work. All other authors declare no conflict of interest.

expression in EGFR mutants but not in EGFR WT, while TIL activation was associated with higher PD-L1 only in EGFR/KRAS WT.

Conclusions: Our findings demonstrate the unique immune profile of EGFR mutant tumors. The high frequency of inactive TILs could explain the low immunotherapy response rates in these patients, while PD-L1 as a predictive biomarker may reflect the constitutive oncogenic signaling rather than immune signaling, which would be associated with high PD-L1 levels and TILs activation.

Keywords

egfr; mutation; PD-L1; TILs; NSCLC

INTRODUCTION

One of the highest impact breakthroughs of the last few years was the introduction of immune checkpoint inhibitors in the treatment of Non-Small Cell Lung Cancer (NSCLC). The impressive clinical activity and duration of response seen in some of the patients with tumors expressing programmed death ligand-1 (PD-L1), the cognate ligand of programmed death 1 (PD-1), an immune checkpoint receptor of tumor infiltrating lymphocytes (TIL), has led to approval of these agents for early NSCLC treatment lines [1–4]. Even though the role of PD-L1 expression level in NSCLC as a predictive biomarker is controversial, tumor PD-L1 expression has been shown to predict up to a 3-fold increase in response to therapy compared with non-expressers [5, 6].

Two mechanisms of PD-L1 upregulation have been proposed [7]. The first mechanism is the induction of PD-L1 expression in tumors as an adaptive immune resistance to local inflammatory signals. The tumor predominantly in response to Interferon gamma (IFNγ) secreted by tumor antigen-specific T cells, induces the expression of PD-L1 by stimulating JAK/STAT pathway [8, 9]. The second mechanism is a result of constitutive oncogenic signaling. Preclinical studies suggest that aberrant oncogenic EGFR and ALK signaling may induce intrinsic PD-L1 upregulation in NSCLC [10, 11]. The exact mechanism of oncogenic PD-L1 induction is still unclear but evidence so far suggests that and MEK/ERK pathway and PI3K/AKT through dysfunction of phosphatase and tensin homolog (PTEN) may be involved [11–14] . This proposed mechanism of PD-L1 upregulation is further supported by the lower clinical response rates to PD-L1 axis inhibitors across trials in patients with NSCLC, whose tumors harbored EGFR mutation with a trend towards lack of a survival benefit over salvage chemotherapy in two phase III trials [1, 3]. This observation suggests that PD-L1 expression may not have uniform predictive value and that PD-L1 oncogenic upregulation may be less predictive than upregulation mediated by immune infiltration. The presence of multiple mechanism for PD-L1 expression may also explain the conflicting data regarding the correlation of PD-L1 and EGFR mutation status. Several studies have shown a positive correlation between EGFR mutations and PD-L1 overexpression [10, 15], while others have shown the opposite or no correlation at all [16–18]. When comparing studies by patient populations (Asian or Caucasian only), there is still no consensus regarding the association of PD-L1 expression and EGFR mutation status, while PD-L1 expression rate and the frequency of *PD-L1* polymorphisms may differ [19, 20].

In contrast, the presence of KRAS mutations appears to be associated with durable clinical response to PD-1 axis agents, possibly due to its association with smoking, and the presence of higher somatic mutation burden and neo-antigen density [21]. The presence of KRAS co-mutations also seem to play an important role to this patient subgroup, with KRAS/TP53 co-mutational status correlating with good response rates but KRAS/STK11 with very poor outcome [22, 23]. Interestingly, a recent study showed that KRAS mutations can also result in PD-L1 upregulation through MEK/ERK but not AKT pathway [24].

Similarly, little is known about TILs populations across mutations in NSCLC. No consistent association has been found between increased TILs and benefit from PD-1 axis treatment in NSCLC [25], although in melanoma and colorectal carcinoma the preexistence of CD8+ TILs has been linked to clinical benefit [26, 27].

It is also possible that the functional status, or more specifically absence of information about the functional status of TIL has also clouded the issue of the association between mutation status and PD-1 axis drug response. Recently, our group has defined a method for in situ assessment of TIL activity [28]. This method requires multiplexed measurement of CD3, Ki67 and Granzyme B. Ki67 is measured in CD3+ cells as a marker of T-cell proliferation while Granzyme B measurement in the same compartment reflects the cytotoxic activity of those cells. By this multiplex panel we can define three immune status classes. The type 1 class has low CD3 (or low TILs) and shows no predictive value. The type 2 is defined as high CD3 with low Ki67 and low Granzyme B suggesting an exhausted or dormant immune status. The type 3 is defined by high CD3 with either high Ki67 or high GranzymeB. These are defined as activated TILs, mimicking data from flow cytometric studies in mouse models.

In another previous study from our group [29], Proximity Ligation Assay (PLA) [30] quantified by the AQUA method of automated quantitative immunofluorescence (QIF) [31], was used to detect EGFR and its adaptor protein GRB2 (Growth factor receptor bound protein 2) as a surrogate for EGFR activation. Here, we quantitatively measured PD-L1 in a series of NSCLC cases and we assessed the relationship of PD-L1 expression and mutation status. We then combine this data with assessment of the TILs population and their activation status across mutations and in the context of different upregulation mechanisms in PD-L1 expression across different mutation subgroups.

MATERIALS AND METHODS

Proximity Ligation Assay

Proximity Ligation Assay has previously been described [29]. In short, fresh 5μm tissue microarray (TMA) sections were deparaffinized at 60°C for 30 minutes, incubated in xylene (soaking twice for 20 minutes) and rehydrated with ethanol (twice in 100% ethanol for 1 minute, and then in 70% ethanol for 1 minute). Antigen retrieval was performed in a pressure-boiling container (PT module, LabVision, Fremont, CA) with EDTA buffer (Sigma-Aldrich, St Louis, MO) pH 8.0 for 20 minutes at 97°C. After blocking of endogenous peroxidase with 30% hydrogen peroxide in methanol, slides were incubated with a blocking solution containing 0.3% bovine serum albumin in Tris-buffered saline

solution and 0.05% Tween solution for 30 minutes at room temperature. Slides were then incubated overnight with a cocktail of EGFR (D38B1) rabbit monoclonal antibody (Cell Signaling Technology, Inc.) and anti-GRB2 (clone 81) mouse monoclonal antibody (BD Biosciences). Anti-rabbit MINUS and anti-mouse PLUS PLA probes (1:5 dilution, Duolink, Sigma-Aldrich) were used to incubate the slides for 60 minutes at 37°C. Following a 30 minute incubation with 5X Ligation Stock (1:5 dilution, Duolink, Sigma-Aldrich) and Ligase (1:40 dilution, Duolink, Sigma-Aldrich) at 37°C, Amplification Stock 5X (1:5 dilution, Duolink, Sigma-Aldrich) and Polymerase (1:80 dilution, Duolink, Sigma-Aldrich) were added for 120 minutes at 37°C. To generate an amplified signal, TMA sections were incubated for 60 minutes at room temperature with 5X Detection Stock (1:5 dilution, Duolink, Sigma-Aldrich), which contains oligonucleotides complementary to the Rolling Circle Amplification product conjugated with Horseradish Peroxidase. Cyanine 5 (Cy5) directly conjugated to tyramide (FP1117; Perkin-Elmer) at a 1:50 dilution for 10 minutes was used for signal generation. Conjugated anti-pan cytokeratin eFluor 570 (clone AE1/AE3, eBioscience) was used to demarcate the epithelial compartment. Finally, mounting medium (ProLong Gold; Molecular Probes) containing 4,6-diamidino-2-phenyl-indole (DAPI) was used to detect tissue nuclei. All primary antibodies and the PLA kit are commercially available. To ensure reproducibility, sections from control slides were run alongside each slide staining.

Multiplexed TILs and TILs activation Immunofluorescence Staining

The multiplexing TIL protocol has been presented before [32]. Briefly, fresh TMA cuts were deparaffinized and subjected to antigen retrieval using EDTA buffer (Sigma-Aldrich, St Louis, MO) pH 8.0 for 20minutes at 97° C in a pressure-boiling container (PT module, Lab Vision, Fremont, CA). Slides were then incubated in 30% hydrogen peroxide in methanol for 30 minutes at room temperature and subsequently with a blocking solution containing 0.3% bovine serum albumin in 0.05% Tween solution for 30 minutes. Staining for pan-cytokeratin, CD4, CD8, and CD20 was performed using a sequential multiplexed immunofluorescence protocol with isotype-specific primary antibodies to detect epithelial tumor cells (cytokeratin, clone M3515, 1:100, DAKO), helper T cells (CD4 IgG, 1:100, clone SP35, Spring Bioscience), cytotoxic T cells (CD8 IgG1, 1:250, clone C8/144B, DAKO), and B lymphocytes (CD20 IgG2a, 1:150, clone L26, DAKO). Nuclei were highlighted using 4’,6-Diamidino-2-Phenylindole (DAPI). Secondary antibodies and fluorescent reagents used were goat anti-rabbit Alexa546 (1:100, Invitrogen), anti-rabbit Envision (K4009, DAKO) with biotynilated tyramide/Streptavidine-Alexa750 conjugate (Perkin-Elmer), anti-mouse IgG1 antibody (1:100, eBioscience, CA) with fluorescein-tyramide (Perkin-Elmer), anti-mouse IgG2a antibody (1:200, Abcam, MA) with Cy5-tyramide (Perkin-Elmer). Residual horseradish peroxidase activity between incubations with secondary antibodies was eliminated by exposing the slides twice for seven minutes to a solution containing benzoic hydrazide (0.136 gr) and hydrogen peroxide (50 μl).

Staining for T-cell activation panel included pan-cytokeratin, CD3, Ki67, and Granzyme B and was performed using a similar sequential multiplexed immunofluorescence protocol with isotype-specific primary antibodies to detect epithelial tumor cells (cytokeratin, clone M3515, 1:100, DAKO), T lymphocytes (CD3 IgG, 1:100, clone SP7, Novus biologicals,

CO), Ki67 (IgG1, 1:100, clone MIB-1, DAKO), and Granzyme B (IgG2a, 1:2000, clone 4E6, Abcam). Fresh control slides from morphologically normal human tonsil were included in each staining batch as positive controls and to ensure reproducibility.

PD-L1 Immunofluorescence Staining

Tissue sections were subjected to the same deparaffinization, antigen retrieval, and blocking protocol mentioned above and incubated overnight with a cocktail of the primary target antibody, PD-L1 (9A11, Cell Signaling Technology) mouse monoclonal antibody, and a cytokeratin antibody, rabbit polyclonal cytokeratin antibody (Z0622, Dako). Next, sections were incubated for 60 minutes at room temperature with Alexa 546-conjugated goat anti-rabbit secondary antibody (Molecular Probes, Eugene, OR, USA) diluted 1:100 in mouse EnVision amplification reagent (K4001, Dako). Cyanine 5 (Cy5) directly conjugated to tyramide (FP1117; Perkin-Elmer) at a 1:50 dilution for 10 minutes was used for target detection and ProLong mounting medium (ProLong Gold; Molecular Probes) containing DAPI was used to stain nuclei. Control slides were run for reproducibility alongside each experimental slide-staining run.

Quantitative Immunofluorescence (QIF)

Quantitative measurement of EGFR:GRB2 PLA, PD-L1, TILs markers and TILs activation markers was performed using AQUA (Automated Quantitative Analysis) method (Genoptix Medical Laboratory), quantifying fluorescent signal within subcellular compartments (tumor and stroma), as described previously [31]. For the epithelial markers, EGFR:GRB2 PLA and PD-L1, a tumor mask was created by binarizing the cytokeratin signal and creating an epithelial compartment. In the case of TILs markers, CD3, CD4, CD8 and CD20, the area in which the signal was measured was defined by the DAPI staining. TILs activation markers, Ki67 and Granzyme B, were measured in a dilated CD3 positive compartment, defining the T lymphocytes.

Quantitative immunofluorescence (QIF) score was calculated by dividing the target pixel intensity by the area of the compartment. QIF scores were normalized to the exposure time and bit depth at which the images were captured, allowing scores collected at different exposure times to be comparable. Serial section slides were used for analyzing the staining and protein expression patterns for the different markers. All tumor spots were visually evaluated and cases with staining artifacts or presence of less than 2% compartment area were systematically excluded.

Tissue Microarray and Patient Cohorts

Tissue specimens were prepared in a tissue microarray format as previously described [33]. Representative tumor areas were obtained from formalin-fixed, paraffin-embedded (FFPE) specimens of the primary tumor, and 0.6mm cores from each tumor block were arrayed in a recipient block. FFPE cell line pellets were used as controls. Yale Tissue Microarray YTMA-310, a NSCLC array that consists of 139 tumor cores from patients with different mutation status was constructed after pathology reports from 2011–2013 were retrieved. NSCLC patient cases that had complete surgical resection of primary tumor and subsequently molecular testing for common NSCLC mutations were selected for further

review. The cases that had adequate residual tumor from primary site were selected and cored. YTMA 310 includes 30 EGFR mutant, 43 KRAS mutant, 66 EGFR and KRAS wild type (EGFR/KRAS WT) patient cases as well as 6 cell line cores (HCC193, A431, HT29, SW480, MCF7, H2126).

YTMA-356, is a NSCLC array that consists of primary tumors resected between 2010–2014 from 43 patient cases that received EGFR tyrosine kinase inhibitors at some point after resection. It includes 35 EGFR mutant, 2 KRAS mutant, 4 EGFR/KRAS WT and 2 of unknown mutation status patient cases as well as 14 cell line cores (H820, H1648, H1993, H441, H1299, A431, A549, H2882, HCC193, HT29, PC9, MCF7, SKBR3, H1355).

A serially collected cohort of patient tissues obtained in the Yale Surgical Pathology suite, Yale Cohort A, comprises a sample collection from 516 NSCLC patients that had surgical resection of their primary tumor between 1988 and 2011. From this cohort, only the patients with follow up information were assessed for EGFR:GRB2 PLA and PD-L1 expression. Clinico-pathological information from patients in the cohort was collected from clinical records and pathology reports. Detailed characteristics of the cohorts' cases that were used are presented in Table 1. All tissue was used after approval from the Yale Human Investigation Committee protocol #9505008219, which approved the patient consent forms or in some cases waiver of consent.

Statistical Analysis

To correlate QIF scores with EGFR mutation, EGFR:GRB2 PLA status, TILs markers' expression and TILs activation status, p-values were calculated by Mann-Whitney analysis. Each patient case was represented by two cores of 0.6mm each and for statistical analysis, the maximal marker score obtained from the two available cores of each case was used. For further statistical analysis, the patient cases included in YTMA 310 and YTMA 356 were combined and treated as one cohort, in order to increase statistical power.

Stratification of the cohort patients according to the markers' levels for survival analysis was performed by obtaining the QIF scores of the patient cohorts and splitting them by median value. Patient characteristics were compared using chi-square test as categorical variables. Overall-survival curves were constructed using the Kaplan-Meier analysis with a follow up of 60 months and statistical significance was determined using the log-rank test. Multivariable Cox proportional hazards models including age, gender, smoking status, histology and clinical stage as co-variables were performed to determine which factors had a significant impact on overall survival and assess the independent prognostic significance of EGFR:GRB2 PLA and PD-L1 expression.

TILs activation subgroups were defined by median cutpoint of CD3, Ki67 and Granzyme B. More specifically, Group 1 includes all patients with low CD3 expression (lower than CD3 median of YTMA 310 and YTMA 356). Group 2 includes patients with high CD3 expression (higher than median) but both Ki67 and Granzyme B low levels (lower than median for each of the markers). Group 3 includes patients with high CD3 expression (higher than median) and high Ki67 or Granzyme B (higher than median for any of the markers).

All p-values were based on two-sided tests and any p-value <0.05 was considered statistically significant. Statistical analyses were performed using JMP Pro software (version 11.2.0, 2014, SAS Institute Inc, Cary, NC) and GraphPad Prism v6.0 for Windows (GraphPad Software, Inc, San Diego, CA).

RESULTS

The relationship between PD-L1 and EGFR:GRB2 co-localization and mutation status in NSCLC patients

The relationship between PD-L1, EGFR mutation status and EGFR:GRB2 complex abundance was evaluated in over 150 NSCLC patient tumor cores with known mutation status. Representative images of two NSCLC cases are shown, that have high EGFR:GRB2 PLA and high PD-L1 expression (Figure S1A, S1B). To determine if specific site mutations were associated with PD-L1 expression, we assessed PD-L1 expression split by mutation site and gene. PD-L1 tumor expression was statistically significantly lower in patient cases with EGFR mutation compared to EGFR/KRAS WT cases ($p<0.0001$) and KRAS mutant cases ($p=0.0009$). Similarly, PD-L1 stroma expression was lower in EGFR mutant cases compared to EGFR/KRAS WT and KRAS mutant cases ($p<0.0001$ and $p=0.0001$, respectively) (Figure 1A-B).

In order to assess the EGFR oncogenic pathway relationship with PD-L1 expression, we used EGFR:GRB2 PLA as a surrogate to EGFR activation. Tumor but not stromal PD-L1 expression was found to be higher in the patient cases with strong EGFR:GRB2 PLA signal ($p=0.03$), consistent with previous reports suggesting that EGFR pathway may have a significant role in the upregulation of PD-L1 in NSCLC tumors (Figure 1C-D). To confirm our findings we used a second independent NSCLC cohort, Yale Cohort A, that included 299 patient cases with evaluable tissue and QIF scores for both (PD-L1 and EGFR:GRB2 PLA) markers. PD-L1 tumor expression was again significantly higher in the high PLA group ($p<0.0001$) (Fig 1E). Furthermore, stratification of patients by both PD-L1 tumor expression and EGFR activation for survival analysis resulted in four distinct patient groups: a group with low PD-L1 expression and low EGFR:GRB2 PLA, a group with high PD-L1 expression and low EGFR:GRB2 PLA, a group of low PD-L1 expression and high EGFR:GRB2 PLA and a group with both high PD-L1 expression and EGFR:GRB2 signaling complexes abundance. High tumor PD-L1 with strong EGFR activation was statistically significantly associated with longer 5-year survival rate compared to the group classified as low for both tumor PD-L1 and EGFR:GRB2 PLA (log-rank $p=0.008$, HR=0.54, 95% CI: 0.34–0.85) (Figure 1F). The groups that had high expression of only one of the markers did not show any difference in survival compared to the other patient subgroups. Detailed characteristics of the cohorts' cases that were used are presented in Table 1. The correlation between PD-L1 and EGFR:GRB2 stratification and patient characteristics including age, gender, stage, tumor histology and smoking status showed no consistent association between PD-L1/EGFR:GRB2 levels and major clinic-pathological variables (Suppl. Table S1).

Multivariate Cox proportional hazards regression analysis was performed to derive risk estimates related to survival for all clinic-pathologic characteristics and PD-L1/EGFR:GRB2

expression (Suppl. Table S2). Cases with missing values were excluded from analysis. High PD-L1/EGFR:GRB2 PLA group was independently associated with better survival in Yale cohort A. As expected, gender and stage were also shown to be independent prognostic markers.

TILs populations across NSCLC mutations

In order to characterize the TILs populations across different mutations we measured CD4, CD8, CD20 and CD3 expression in the NSCLC cohort (YTMA 310 and YTMA 356) with known mutation status. Interestingly, CD4+ expression, reflecting the presence of T-helper cells, was significantly higher in KRAS mutant cases compared to EGFR/KRAS WT (p=0.0029), while the difference with EGFR mutant cases was close to significant (p=0.06) (Figure 2A). Similarly, for the CD8+ expression (cytotoxic T-cells), KRAS mutant cases had higher expression levels compared to both EGFR mutant cases (p=0.01) and EGFR/KRAS WT (p=0.07) (Figure 2B). The presence of higher levels of CD4+ and CD8+ in patients with KRAS mutation suggests a more inflamed profile of this patient subgroup, compared to EGFR mutants or EGFR/KRAS WT patients. The presence of tertiary lymphoid structures has been implicated to play a role in a number of cancer types [34–36], including NSCLC. In our patient population, we measured CD20+ expression as a marker assessing the presence of B-cells in the tumor microenvironment. CD20+ cell expression was significantly lower in EGFR/KRAS WT patients compared to EGFR mutant (p=00026) and KRAS mutant (p=0.01) patients. Finally, for CD3+ expression although there was a trend, the difference between KRAS mutants and the other mutation subgroups was not significant (Figure 2D). Representative images of multiplexed TILs markers' staining pattern are shown in Suppl. Figure S1C-D.

The most common and well-documented mutations, constituting 80–90% of all EGFR mutations in NSCLC [37, 38], are in-frame deletions in exon 19, which eliminate the conserved motif LREA (residues 747–750), and the exon 21 L858R substitution [39]. Those two major EGFR mutation sites have been shown to have biological differences with the exon 19 deletions being associated with higher sensitivity to EGFR tyrosine kinase inhibitors and longer OS [40]. In our study, we found that there is a difference in the immune profile of those EGFR mutation sites. Exon 21 L858R group were more inflamed tumors compared to exon 19 deletions, with a trend towards higher CD4+ expression (p=0.11) (Figure 2E) and a significantly higher CD8+ expression (p=0.03) (Figure 2F). While there was no significant difference in CD20+ expression, there was a trend (p=0.11) towards higher CD3+ expression in exon 21 L858R group (Figure 2G and 2H respectively).

TILs activation status across NSCLC mutations

Activation state of TILs is often assessed by flow cytometry, but is more challenging in FFPE specimens. In a previous report from our group (Gettinger et al, in pres*s*) we showed that 3 different TILs activation subgroups can be defined in NSCLC patients by the expression of Ki67, a marker of proliferation, and Granzyme B, a marker reflecting the levels of the cytotoxic granules. Based on the expression of those markers specifically in CD3+ T-cells, patients can be classified as having low CD3+ T-cell expression to the tumor microenvironment (Group 1), high number but inactive CD3+ T-cells by low expression of

proliferation (Ki67) and cytotoxicity (Granzyme B) markers (Group 2) and high number and strong activity of CD3+ T-cells by either high proliferation or cytotoxicity markers' expression (Group 3). A representative image of the activation markers' multiplexed IF staining is shown in Suppl. Figure S1D and a schematic of the patient sub-classification by their TILs activation status is shown in Suppl. Figure S2B.

Comparison of tumors split by activation status and mutation status (Figure 3A) shows that TILS, when present in EGFR mutant tumors, are more commonly inactive (16 cases in group 2 compared to 10 in group 3, 28.6% and 17.8% respectively). This low immunogenicity was exclusive to EGFR mutant patients, with EGFR/KRAS WT having a much lower percentage (9.1%, n=5/55) of patients belonging to activation group 2. For KRAS mutant patients, the TILs activation profile was completely reversed, with the majority of patients (51.4%, n=19/37) being classified as group 3 (active T-cells) and only 1 patient out of the 37 having inactive CD3+ cells.

To complement and confirm the activation status of T-cells, we compared tumor and stroma PD-L1 expression across TILs activation subgroups (Figure 3B and 3C). Group 3 (active T-cells) was statistically significantly associated with higher tumor (p=0.0014) and stroma (p=0.02) PD-L1 expression compared to Group 2 and Group 1 (p=0.006 and p=0.0001, respectively). This finding is consistent with the induction of PD-L1 expression in NSCLC as an adaptive immune resistance mechanism to local inflammatory signals.

When comparing EGFR mutation hotspots (Figure 3D), the number of cases in each group for exon 19 deletions was: 14/22 in group 1, 6/22 in group 2 and 2/22 patients in group 3. For exon 21 L858R substitutions there were 11/24 in group 1, 7/24 in group 2 and 6/24 in group 3. Both tumors harboring exon 19 deletions and exon 21 L858R had a high number of cases with inactive T-cells (group 2) when TILs were present (n=6/8 and n=7/13 respectively). Interestingly, for group 3 (tumors with activated T-cells) the number of patients was higher among the exon 21 L858R substitution compared to exon 19 deletion group (n=6/24 and n=2/22 respectively), a finding that was consistent with the elevated TILs markers expression in this subgroup. While there was a difference in the immune profile, PD-L1 tumor and stroma expression (Figure 3E and 3F) was comparable between the two EGFR mutation sites.

PD-L1 upregulation mechanisms across mutations

Previous findings have indicated that both high EGFR oncogenic signaling and IFNγ expression are associated with high PD-L1 tumor expression [7], though the dependence on each of the two upregulation mechanisms is still unclear. In order to identify whether either is associated with mutation status, we compared PD-L1 tumor expression in each mutation group by both TILs activation and EGFR pathway activation. In EGFR mutant patients, Group 3 TILs activation was not associated with higher PD-L1 expression (Figure 4A). Conversely, high EGFR activation by EGFR:GRB2 PLA, was statistically significantly correlated with the higher PD-L1 expression (p=0.0025) (Fig 4B). In EGFR/KRAS WT patients, only TILs activation had a statistically significant correlation with PD-L1 expression (p=0.012) (Figure 4E), while EGFR activation was not associated with higher PD-L1 tumor expression (Figure 4F). In KRAS mutant patients none of the suggested

upregulation mechanisms was correlated with high PD-L1 expression, suggesting that PD-L1 regulation is not clearly dependent on any of these upregulation mechanisms (Figure 4C and 4D).

DISCUSSION

NSCLC is one of the malignancies with the highest mutational burden [41]. It has been demonstrated that the mutational landscape and neo-antigens increase the response rate to PD-1 [21] axis inhibitors. In the case of EGFR mutant tumors, even though the mutational burden is low, PD-L1 expression has been reported to be high [10] in some cases, suggesting a regulation mechanism mediated by the EGFR oncogenic signaling pathway, rather than an adaptive process by induction with local inflammatory signals [7]. In previous studies [29, 42], it was shown that detection of the EGFR and GRB2 complexes by PLA is indicative of the receptor's activation and it is independent of the overall EGFR expression and mutation status.

PD-L1 expression as a biomarker to PD-1 axis treatment is far from optimal. Efforts for the discovery of new markers and assays that would improve patient selection are ongoing. Tumor Mutation Burden (TMB), a method of measurement of total number of mutations per tumor genome coding area, has shown promising results as a predictive biomarker to immunotherapy in advanced cancers [43, 44], including NSCLC for first line treatment with nivolumab plus ipilimumab [45]. Similarly, the development of effector T-cell gene expression (Teff GE) signatures can successfully select subgroups of patients with improved benefit [46–49]. Further standardization though is needed before those novel approaches can be implemented in clinical practice.

Currently, PD-L1 expression remains the most widely used biomarker for selection of responders to PD-1/PD-L1 checkpoint inhibitors even though many patients, even in the lower tumor PD-L1 expression subgroups have shown response [50]. One possible explanation could be the biological role of PD-L1 itself, since as a cancer immune escape mechanism it could indicate immune pressure by tumor microenvironment and consequently indirectly predict the efficacy of the PD-1 axis treatment. However, PD-L1 expression has been shown to be also associated with EGFR oncogenic signaling activity that is independent of the immune pressure. In this case, PD-L1 expression would not necessarily reflect TILs potential activity in the tumor microenvironment.

Recent data suggest that EGFR mutated patients are less likely to benefit from PD-1 axis blockade. A recent meta-analysis [51] that included randomized clinical trials comparing nivolumab, pembrolizumab, or atezolizumab with docetaxel reported that checkpoint inhibitors didn't offer any survival benefit for the patients with EGFR mutant tumors and interestingly and there was a trend (not reaching statistical significance) towards worse OS (HR: 1.11, 95% CI 0.80–1.53). In this meta-analysis though, PD-L1 expression was not used to further stratify patients carrying EGFR mutations. Similarly, another retrospective study [16], reported a negative association between EGFR mutation and response rates to PD-1/PD-L1 inhibitors. In the same study, PD-L1 expression was lower in the EGFR mutant group compared to a control KRAS mutant patient group, although the difference was not

statistically significant due to limited power. However, in a recent phase 3 clinical trial, patients with EGFR and ALK genetic alterations showed improved PFS (HR:0.59, 95% CI: 0.37–0.94) and 46% reduction in the risk of death (HR:0.54, 95% CI: 0.29–1.03) in the group receiving atezolizumab, carboplatin, paclitaxel and bevacizumab vs the group that received only chemotherapy with bevacizumab and the benefit was observed despite lower PD-L1 expression in this population [46, 47]. This study highlights the importance of combination treatment, especially in patients that would not benefit with single checkpoint inhibition and the urgency to elucidate pathways' crosstalk and biomarker correlations that could generate hypotheses for future clinical trials.

Here, we showed that PD-L1 expression was significantly lower in EGFR mutant NSCLC patients compared to EGFR/KRAS WT and KRAS mutant patients. While both EGFR signaling activation and immune pressure were associated with higher PD-L1 tumor expression as suggested upregulation mechanisms, in the EGFR mutant patient group, only EGFR activation was associated with high PD-L1 expression, while T-cells in most patient cases were inactive as defined by low proliferation and cytotoxicity marker expression. This suggests that PD-L1 expression in this mutation subgroup probably only reflects the oncogenic, EGFR driven PD-L1 expression rather than the underlying T-cell activity. This observation provides a potential explanation for lack of response in PD-1 axis inhibitor trials even with high PD-L1 expression. Additionally, in our study, stratification of patients by PD-L1 expression and EGFR activation, showed different survival rates between subgroups. Further research is required to study potential synergistic activity of those markers.

Previous studies on KRAS mutant tumors have attempted to compare immune markers' expression and TILs populations to other genomic alteration patient groups. A recent study reported a high prevalence of concurrent PD-L1 expression and abundant CD8+ TILs in KRAS mutants [52]. The high CD8+ abundance in this group compared to EGFR mutant patients was further confirmed by Busch at al [53]. Conversely, other studies have failed to show any correlation between KRAS mutation and immunophenotype [54, 55]. In our study, we saw a significantly higher immune response of the KRAS mutant patients compared to EGFR mutants and EGFR/KRAS WT. It is unclear though, whether this difference in immunogenicity is due to the mutation itself or the high neo-antigen presence, while the presence of KRAS co-mutations was not assessed in our study. PD-L1 expression was also found to be high in KRAS mutant tumors but there was no statistically significant association with activated TILs or EGFR activation. Chen et al. [24] reported that KRAS mutant tumors could also result in PD-L1 upregulation through ERK pathway in NSCLC. Thus, although the inflamed profile of KRAS mutant tumors suggests that PD-L1 could be a induced as an acquired immune resistance mechanism, in our study we did not find any clear association with either PD-L1 upregulation mechanisms even though EGFR:GRB2 PLA assay would not be able to assess accurately KRAS oncogenic PD-L1 induction. In any case, the KRAS mutant patient group could be a good candidate for any immune therapy that would potentially increase T-cell efficacy, by blocking immune escape mechanisms.

There are several limitations to this study. The most significant is that the cohort did not include any patients treated with PD-1 axis inhibitors. Thus, we were unable to evaluate the predictive potential of the assay and whether PD-L1 expression correlated with any of the

suggested upregulation mechanisms would increase the predictive value of PD-L1. A second limitation is the fact that the assays were done entirely on tissue microarrays. Immune marker assessment in the setting of TMAs can challenging due to the high heterogeneity, especially with markers like PD-L1. For this study, we used two TMA cores representing each patient to minimize sampling errors. While tissue microarrays are often used for large cohort studies, and considered representative, they are never used in a true clinical setting. However, in other studies [56], we have shown that whole slides can be easily measured using quantitative fluorescence in the same manner used here for tissue microarrays. Studies are underway to determine the area of tumor needed to represent TILs and to predict response to PD-1 axis therapy.

In conclusion, there is significant difference of the immune cell populations across mutations and EGFR mutation sites in NSCLC, with PD-L1 expression having stronger association with different upregulation mechanisms in each mutation group. We hope that after further validation on clinical trial tissue, this tool, or similar proximity tool, could provide a method to further classify PD-L1 tumor expression to EGFR signaling activity and TILs activity and guide therapeutic decisions in tumor mutation subgroups.

Supplementary Material

Refer to Web version on PubMed Central for supplementary material.

Acknowledgments:

The authors acknowledge the expert assistance of Lori Charette and her staff in the Yale Tissue Microarray Facility division of Yale Pathology Tissue Services for construction of the tissue microarrays used in the study.

Additional Information: This work was supported by grants from the NIH including the Yale SPORE in Lung Cancer, P50-CA196530, Stand Up to Cancer and the OKIBEE support grant (KS).

REFERENCES

1. Borghaei H, Paz-Ares L, Horn L, et al. Nivolumab versus Docetaxel in Advanced Nonsquamous Non-Small-Cell Lung Cancer. N Engl J Med 2015;373:1627–1639. [PubMed: 26412456]
2. Brahmer J, Reckamp KL, Baas P, et al. Nivolumab versus Docetaxel in Advanced Squamous-Cell Non-Small-Cell Lung Cancer. The New England journal of medicine 2015;373:123–135. [PubMed: 26028407]
3. Herbst RS, Baas P, Kim DW, et al. Pembrolizumab versus docetaxel for previously treated, PD-L1-positive, advanced non-small-cell lung cancer (KEYNOTE-010): a randomised controlled trial. Lancet 2016;387:1540–1550. [PubMed: 26712084]
4. Reck M, Rodriguez-Abreu D, Robinson AG, et al. Pembrolizumab versus Chemotherapy for PD-L1-Positive Non-Small-Cell Lung Cancer. The New England journal of medicine 2016;375:1823–1833. [PubMed: 27718847]
5. Brahmer JR, Tykodi SS, Chow LQ, et al. Safety and activity of anti-PD-L1 antibody in patients with advanced cancer. The New England journal of medicine 2012;366:2455–2465. [PubMed: 22658128]
6. Topalian SL, Hodi FS, Brahmer JR, et al. Safety, activity, and immune correlates of anti-PD-1 antibody in cancer. The New England journal of medicine 2012;366:2443–2454. [PubMed: 22658127]
7. Pardoll DM. The blockade of immune checkpoints in cancer immunotherapy. Nat Rev Cancer 2012;12:252–264. [PubMed: 22437870]

8. Bellucci R, Martin A, Bommarito D, et al. Interferon-gamma-induced activation of JAK1 and JAK2 suppresses tumor cell susceptibility to NK cells through upregulation of PD-L1 expression. Oncoimmunology 2015;4:e1008824. [PubMed: 26155422]

9. Ribas A Adaptive Immune Resistance: How Cancer Protects from Immune Attack. Cancer Discov 2015;5:915–919. [PubMed: 26272491]

10. Akbay EA, Koyama S, Carretero J, et al. Activation of the PD-1 pathway contributes to immune escape in EGFR-driven lung tumors. Cancer Discov 2013;3:1355–1363. [PubMed: 24078774]

11. Ota K, Azuma K, Kawahara A, et al. Induction of PD-L1 Expression by the EML4-ALK Oncoprotein and Downstream Signaling Pathways in Non-Small Cell Lung Cancer. Clin Cancer Res 2015;21:4014–4021. [PubMed: 26019170]

12. Jiang X, Zhou J, Giobbie-Hurder A, et al. The activation of MAPK in melanoma cells resistant to BRAF inhibition promotes PD-L1 expression that is reversible by MEK and PI3K inhibition. Clin Cancer Res 2013;19:598–609. [PubMed: 23095323]

13. Parsa AT, Waldron JS, Panner A, et al. Loss of tumor suppressor PTEN function increases B7-H1 expression and immunoresistance in glioma. Nat Med 2007;13:84–88. [PubMed: 17159987]

14. Crane CA, Panner A, Murray JC, et al. PI(3) kinase is associated with a mechanism of immunoresistance in breast and prostate cancer. Oncogene 2009;28:306–312. [PubMed: 18850006]

15. Azuma K, Ota K, Kawahara A, et al. Association of PD-L1 overexpression with activating EGFR mutations in surgically resected nonsmall-cell lung cancer. Annals of oncology : official journal of the European Society for Medical Oncology / ESMO 2014;25:1935–1940.

16. Gainor JF, Shaw AT, Sequist LV, et al. EGFR Mutations and ALK Rearrangements Are Associated with Low Response Rates to PD-1 Pathway Blockade in Non-Small Cell Lung Cancer (NSCLC): A Retrospective Analysis. Clin Cancer Res 2016.

17. Zhang Y, Wang L, Li Y, et al. Protein expression of programmed death 1 ligand 1 and ligand 2 independently predict poor prognosis in surgically resected lung adenocarcinoma. OncoTargets and therapy 2014;7:567–573. [PubMed: 24748806]

18. Yang CY, Lin MW, Chang YL, et al. Programmed cell death-ligand 1 expression in surgically resected stage I pulmonary adenocarcinoma and its correlation with driver mutations and clinical outcomes. Eur J Cancer 2014;50:1361–1369. [PubMed: 24548766]

19. Nomizo T, Ozasa H, Tsuji T, et al. Clinical Impact of Single Nucleotide Polymorphism in PD-L1 on Response to Nivolumab for Advanced Non-Small-Cell Lung Cancer Patients. Sci Rep 2017;7:45124. [PubMed: 28332580]

20. Lin Z, Xu Y, Zhang Y, et al. The prevalence and clinicopathological features of programmed death-ligand 1 (PD-L1) expression: a pooled analysis of literatures. Oncotarget 2016;7:15033–15046. [PubMed: 26930715]

21. Rizvi NA, Hellmann MD, Snyder A, et al. Cancer immunology. Mutational landscape determines sensitivity to PD-1 blockade in non-small cell lung cancer. Science 2015;348:124–128. [PubMed: 25765070]

22. Skoulidis F, Byers LA, Diao L, et al. Co-occurring genomic alterations define major subsets of KRAS-mutant lung adenocarcinoma with distinct biology, immune profiles, and therapeutic vulnerabilities. Cancer Discov 2015;5:860–877. [PubMed: 26069186]

23. Skoulidis F, Hellmann MD, Awad MM, et al. STK11/LKB1 co-mutations to predict for de novo resistance to PD-1/PD-L1 axis blockade in KRAS-mutant lung adenocarcinoma. Journal of Clinical Oncology 2017;35:9016–9016.

24. Chen N, Fang W, Lin Z, et al. KRAS mutation-induced upregulation of PD-L1 mediates immune escape in human lung adenocarcinoma. Cancer Immunol Immunother 2017;66:1175–1187. [PubMed: 28451792]

25. Herbst RS, Soria JC, Kowanetz M, et al. Predictive correlates of response to the anti-PD-L1 antibody MPDL3280A in cancer patients. Nature 2014;515:563–567. [PubMed: 25428504]

26. Tumeh PC, Harview CL, Yearley JH, et al. PD-1 blockade induces responses by inhibiting adaptive immune resistance. Nature 2014;515:568–571. [PubMed: 25428505]

27. Le DT, Uram JN, Wang H, et al. PD-1 Blockade in Tumors with Mismatch-Repair Deficiency. The New England journal of medicine 2015;372:2509–2520. [PubMed: 26028255]

28. Schalper KA, Mani N, Toki M, et al. Clinical value of measuring T-cell activation and proliferation using multiplexed quantitative fluorescence in non-small cell lung cancer (NSCLC). Journal of Clinical Oncology 2016;34:11610–11610.
29. Toki MI, Carvajal-Hausdorf DE, Altan M, et al. EGFR-GRB2 Protein Colocalization Is a Prognostic Factor Unrelated to Overall EGFR Expression or EGFR Mutation in Lung Adenocarcinoma. Journal of thoracic oncology : official publication of the International Association for the Study of Lung Cancer 2016;11:1901–1911.
30. Soderberg O, Gullberg M, Jarvius M, et al. Direct observation of individual endogenous protein complexes in situ by proximity ligation. Nature methods 2006;3:995–1000. [PubMed: 17072308]
31. Camp RL, Chung GG, Rimm DL. Automated subcellular localization and quantification of protein expression in tissue microarrays. Nature medicine 2002;8:1323–1327.
32. Brown JR, Wimberly H, Lannin DR, et al. Multiplexed quantitative analysis of CD3, CD8, and CD20 predicts response to neoadjuvant chemotherapy in breast cancer. Clinical cancer research : an official journal of the American Association for Cancer Research 2014;20:5995–6005. [PubMed: 25255793]
33. McCabe A, Dolled-Filhart M, Camp RL, et al. Automated quantitative analysis (AQUA) of in situ protein expression, antibody concentration, and prognosis. Journal of the National Cancer Institute 2005;97:1808–1815. [PubMed: 16368942]
34. Fridman WH, Pages F, Sautes-Fridman C, et al. The immune contexture in human tumours: impact on clinical outcome. Nature reviews Cancer 2012;12:298–306. [PubMed: 22419253]
35. Gu-Trantien C, Loi S, Garaud S, et al. CD4(+) follicular helper T cell infiltration predicts breast cancer survival. J Clin Invest 2013;123:2873–2892. [PubMed: 23778140]
36. Di Caro G, Bergomas F, Grizzi F, et al. Occurrence of tertiary lymphoid tissue is associated with T-cell infiltration and predicts better prognosis in early-stage colorectal cancers. Clinical cancer research : an official journal of the American Association for Cancer Research 2014;20:2147–2158. [PubMed: 24523438]
37. Sharma SV, Bell DW, Settleman J, et al. Epidermal growth factor receptor mutations in lung cancer. Nature Reviews Cancer 2007;7:169–181. [PubMed: 17318210]
38. Sakurada A, Shepherd FA, Tsao MS. Epidermal growth factor receptor tyrosine kinase inhibitors in lung cancer: Impact of primary or secondary mutations. Clinical lung cancer 2006;7:S138–S144. [PubMed: 16764754]
39. Eberhard DA, Johnson BE, Amler LC, et al. Mutations in the epidermal growth factor receptor and in KRAS are predictive and prognostic indicators in patients with non-small-cell lung cancer treated with chemotherapy alone and in combination with erlotinib. Journal of Clinical Oncology 2005;23:5900–5909. [PubMed: 16043828]
40. Lee CK, Wu YL, Ding PN, et al. Impact of Specific Epidermal Growth Factor Receptor (EGFR) Mutations and Clinical Characteristics on Outcomes After Treatment With EGFR Tyrosine Kinase Inhibitors Versus Chemotherapy in EGFR-Mutant Lung Cancer: A Meta-Analysis. J Clin Oncol 2015;33:1958–1965. [PubMed: 25897154]
41. Alexandrov LB, Nik-Zainal S, Wedge DC, et al. Signatures of mutational processes in human cancer. Nature 2013;500:415–421. [PubMed: 23945592]
42. Smith MA, Hall R, Fisher K, et al. Annotation of human cancers with EGFR signaling-associated protein complexes using proximity ligation assays. Science signaling 2015;8:ra4. [PubMed: 25587191]
43. Snyder A, Makarov V, Merghoub T, et al. Genetic basis for clinical response to CTLA-4 blockade in melanoma. N Engl J Med 2014;371:2189–2199. [PubMed: 25409260]
44. Rosenberg JE, Hoffman-Censits J, Powles T, et al. Atezolizumab in patients with locally advanced and metastatic urothelial carcinoma who have progressed following treatment with platinum-based chemotherapy: a single-arm, multicentre, phase 2 trial. Lancet 2016;387:1909–1920. [PubMed: 26952546]
45. Hellmann MD, Ciuleanu TE, Pluzanski A, et al. Nivolumab plus Ipilimumab in Lung Cancer with a High Tumor Mutational Burden. N Engl J Med 2018;378:2093–2104. [PubMed: 29658845]
46. Socinski MA, Jotte RM, Cappuzzo F, et al. Overall survival (OS) analysis of IMpower150, a randomized Ph 3 study of atezolizumab (atezo) + chemotherapy (chemo) ± bevacizumab (bev) vs

chemo + bev in 1L nonsquamous (NSQ) NSCLC. Journal of Clinical Oncology 2018;36:9002–9002.

47. Socinski MA, Jotte RM, Cappuzzo F, et al. Atezolizumab for First-Line Treatment of Metastatic Nonsquamous NSCLC. N Engl J Med 2018;378:2288–2301. [PubMed: 29863955]
48. Kowanetz M, Zou W, McCleland M, et al. MA 05.09 Pre-Existing Immunity Measured by Teff Gene Expression in Tumor Tissue is Associated with Atezolizumad Efficacy in NSCLC. Journal of Thoracic Oncology 2017;12:S1817–S1818.
49. Fehrenbacher L, Spira A, Ballinger M, et al. Atezolizumab versus docetaxel for patients with previously treated non-small-cell lung cancer (POPLAR): a multicentre, open-label, phase 2 randomised controlled trial. The Lancet 2016;387:1837–1846.
50. Shien K, Papadimitrakopoulou VA, Wistuba, II. Predictive biomarkers of response to PD-1/PD-L1 immune checkpoint inhibitors in non-small cell lung cancer. Lung Cancer 2016;99:79–87. [PubMed: 27565919]
51. Lee CK, Man J, Lord S, et al. Clinical and Molecular Characteristics Associated With Survival Among Patients Treated With Checkpoint Inhibitors for Advanced Non-Small Cell Lung Carcinoma: A Systematic Review and Meta-analysis. JAMA Oncol 2018;4:210–216. [PubMed: 29270615]
52. Huynh TG, Morales-Oyarvide V, Campo MJ, et al. Programmed Cell Death Ligand 1 Expression in Resected Lung Adenocarcinomas: Association with Immune Microenvironment. J Thorac Oncol 2016;11:1869–1878. [PubMed: 27568346]
53. Busch SE, Hanke ML, Kargl J, et al. Lung Cancer Subtypes Generate Unique Immune Responses. J Immunol 2016;197:4493–4503. [PubMed: 27799309]
54. Lizotte PH, Ivanova EV, Awad MM, et al. Multiparametric profiling of non-small-cell lung cancers reveals distinct immunophenotypes. JCI Insight 2016;1:e89014. [PubMed: 27699239]
55. Mansuet-Lupo A, Alifano M, Pecuchet N, et al. Intratumoral Immune Cell Densities Are Associated with Lung Adenocarcinoma Gene Alterations. Am J Respir Crit Care Med 2016;194:1403–1412. [PubMed: 27299180]
56. McLaughlin J, Han G, Schalper KA, et al. Quantitative Assessment of the Heterogeneity of PD-L1 Expression in Non-Small-Cell Lung Cancer. JAMA oncology 2015:1–9.

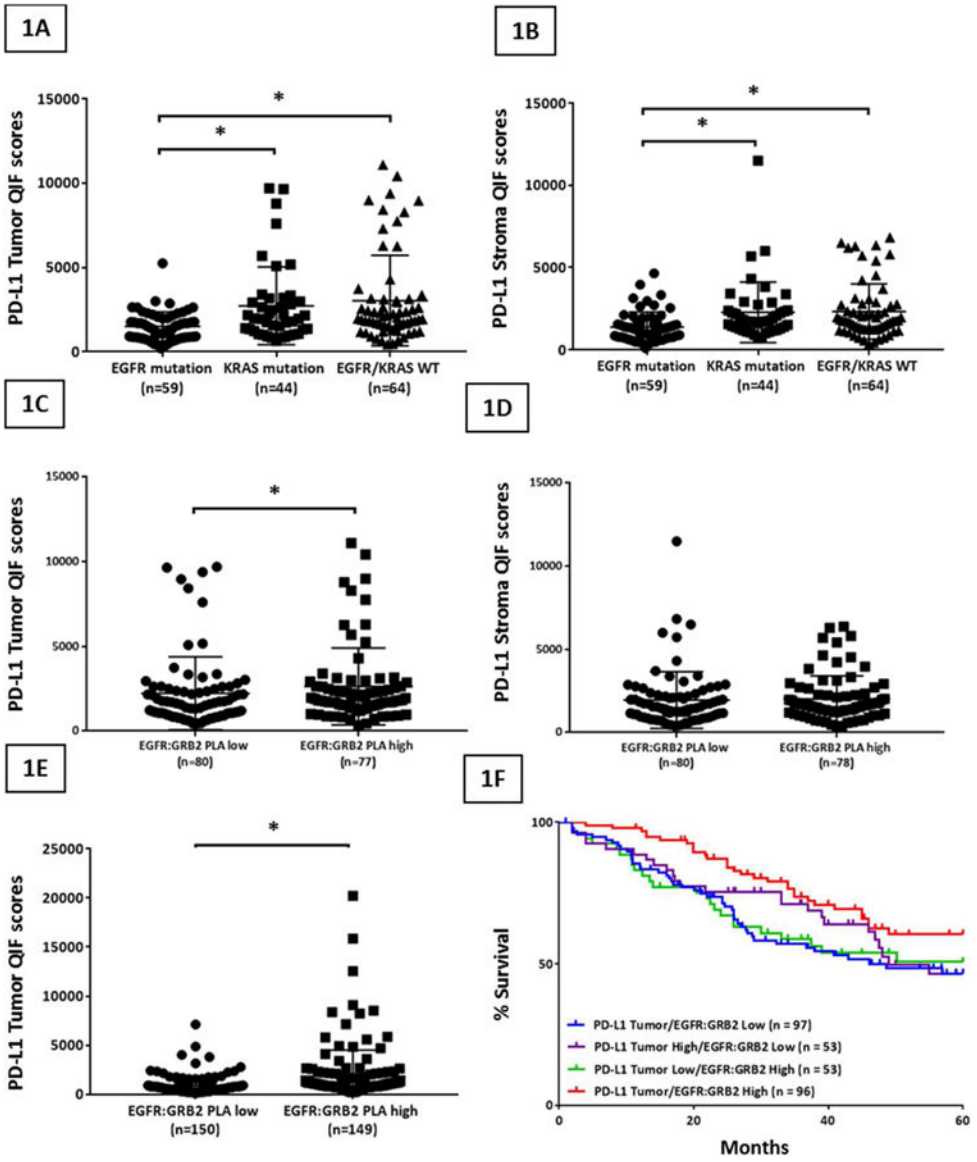

Figure 1: Tumor and stroma PD-L1 expression across mutations and EGFR activation in NSCLC.

(A-B) Tumor and stroma PD-L1 QIF scores in NSCLC tumors with different mutation status. EGFR mutant cases have significantly lower tumor ($p<0.0001$) and stroma ($p<0.0001$) PD-L1 QIF scores compared to EGFR/KRAS wild type and KRAS mutant tumors ($p=0.0009$ and $p=0.0001$, respectively). (C-D) Tumor and stroma PD-L1 QIF scores in NSCLC cases with different EGFR activation status, by EGFR:GRB2 PLA. Tumor ($p=0.03$) PD-L1 QIF scores are significantly higher in the EGFR:GRB2 PLA high patient group. (E) Tumor PD-L1 QIF scores are significantly higher ($p<0.0001$) in the EGFR:GRB2 PLA high patient group in an independent NSCLC cohort. (F) Kaplan-Meier 5-year survival curves of NSCLC patients in Yale cohort A, stratified by tumor PD-L1 and EGFR:GRB2 PLA QIF scores. * Denotes statistical significance $p<0.05$.

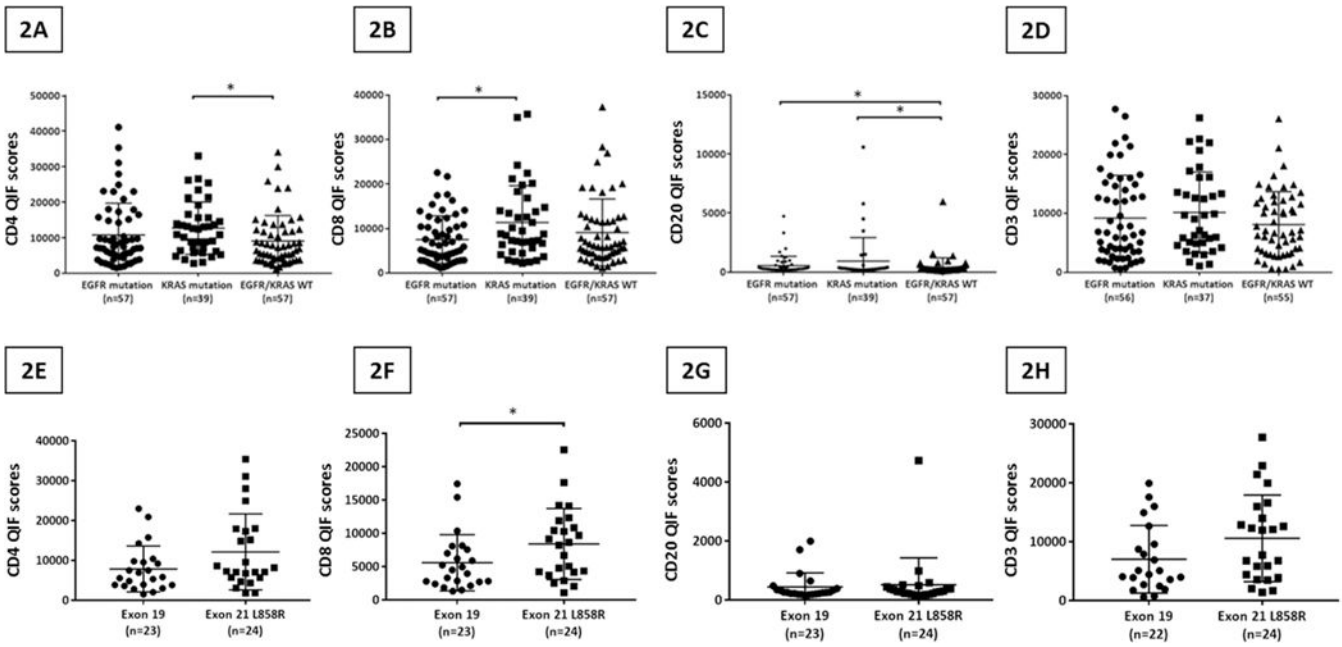

Figure 2: TILs populations in NSCLC cases with different mutation status and EGFR mutation sites.

(A) CD4+ QIF scores are higher in KRAS mutant NSCLC cases (p=0.0029) compared to EGFR/KRAS WT and EGFR mutant cases (p=0.06). (B) CD8+ QIF scores are higher in KRAS mutant NSCLC cases (p=0.01) compared to EGFR mutant cases. (C) CD20+ QIF scores are lower in EGFR/KRAS WT compared to EGFR mutant (p=0.0026) and KRAS mutant (p=0.01) cases. (D) No statistically significant difference across mutations in CD3+ QIF scores. (E) No statistically significant difference across EGFR mutation sites in CD4+ QIF scores. (F) CD8+ QIF scores are higher in tumors with exon 21 L858R substitution (p=0.03) compared to exon 19 deletions. (G) No statistically significant difference across EGFR mutation sites in CD20+ QIF scores. (E) No statistically significant difference across EGFR mutation sites in CD3+ QIF scores.

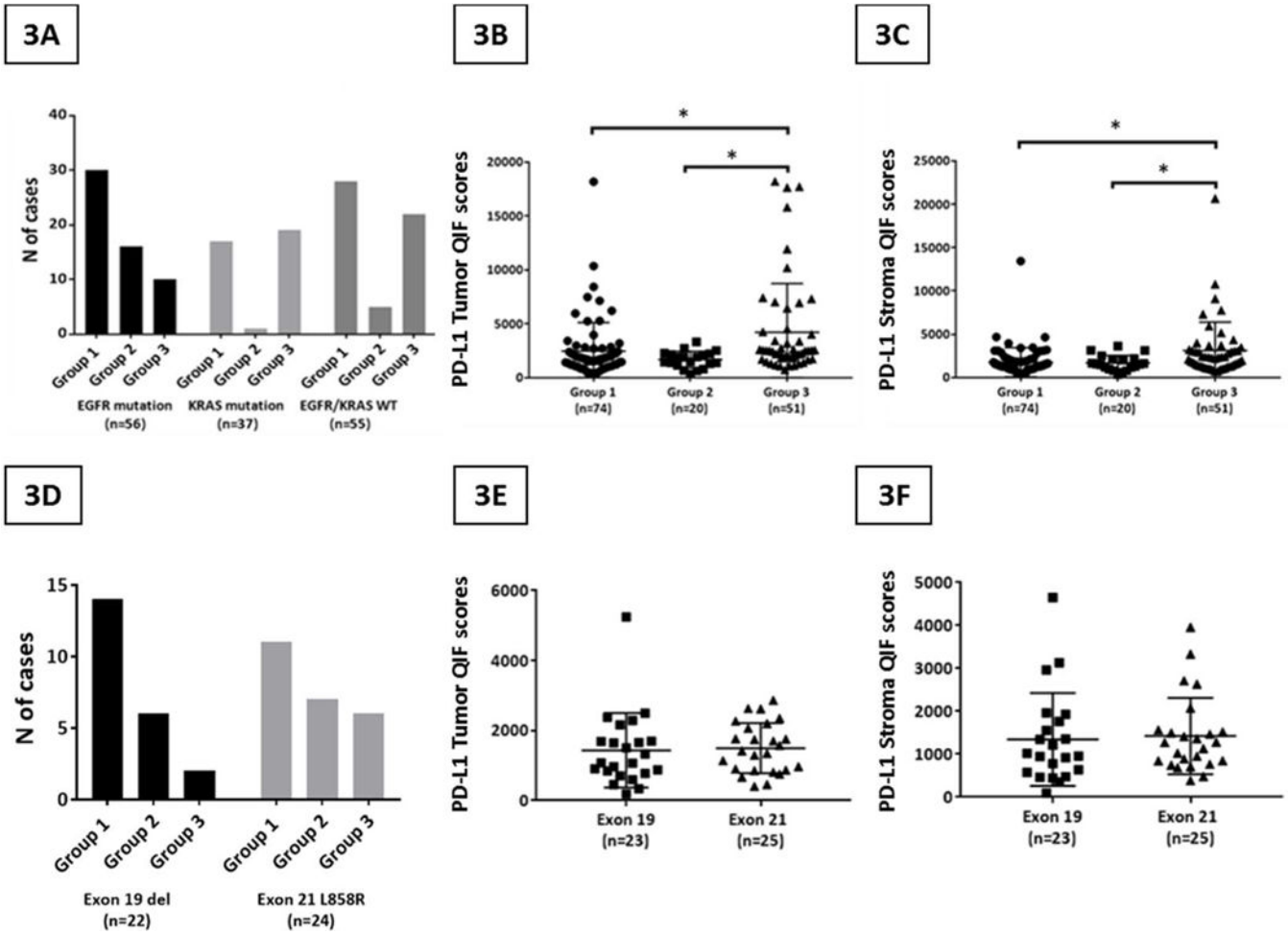

Figure 3: TILs activation status across mutations in NSCLC.

(A) Number of cases in each TILs activation subgroup across mutations in NSCLC. (B) PD-L1 tumor expression in cases stratified by TILs activation status. Group 3 has a significantly higher PD-L1 expression compared to Group 1 (p=0.0006) and Group 2 (p=0.0014). (C) PD-L1 stroma expression in cases stratified by TILs activation status. Group 3 has a significantly higher PD-L1 expression compared to Group 1 (p=0.0001) and Group 2 (p=0.02). (D) Number of cases in each TILs activation subgroup across EGFR mutation sites in NSCLC. (E-F) Tumor and stroma PD-L1 QIF scores in EGFR mutant tumors across mutation sites.

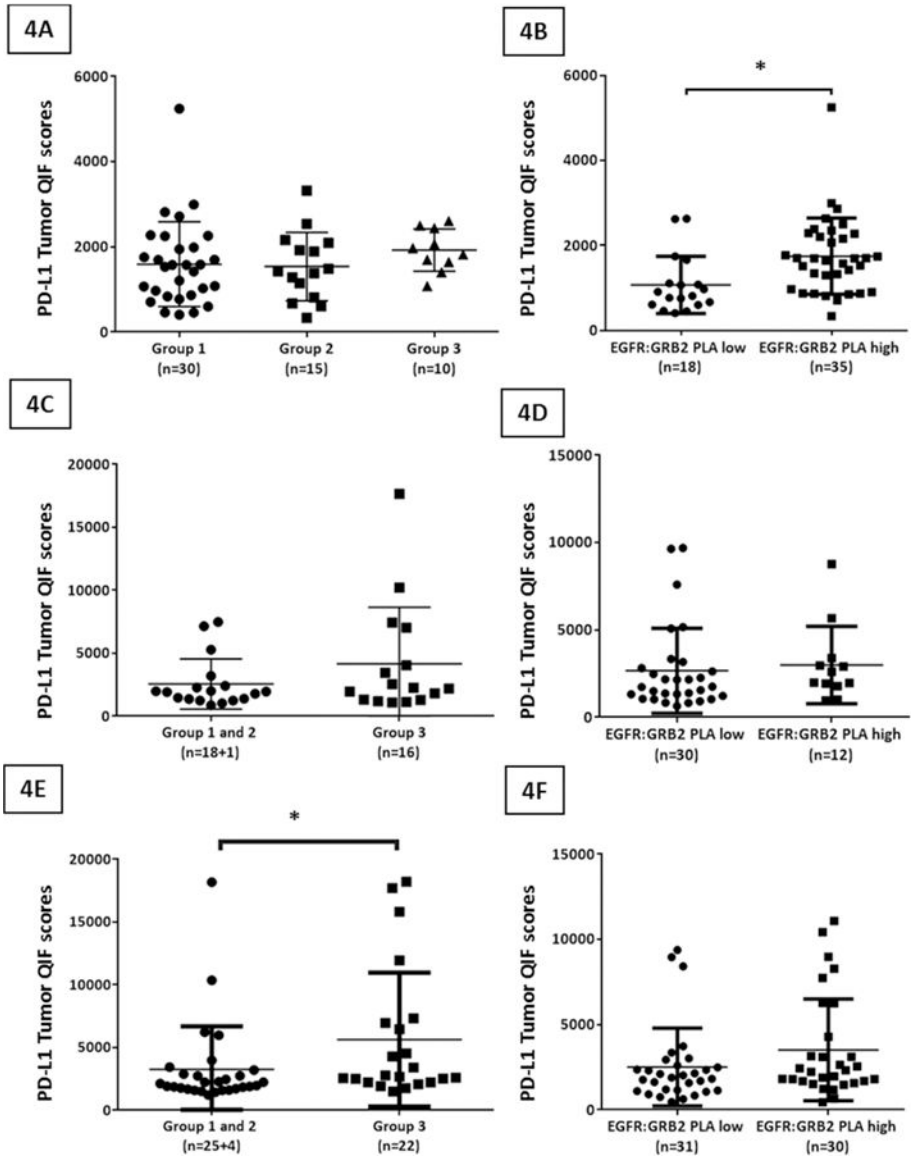

Figure 4: Comparison of PD-L1 tumor upregulation mechanisms across mutations in NSCLC.
(A-B) EGFR mutant cases. No significant difference when cases are stratified by TILs activation status, but there is a statistically significant difference when stratified by their EGFR activation status, high EGFR:GRB2 PLA is associated with higher PD-L1 expression (p=0.0025). (C-D) KRAS mutant cases. No significant difference in PD-L1 expression when cases are stratified by TILs activation status or EGFR activation. (E-F) EGFR/KRAS WT cases. Statistically significant difference (p=0.012) in PD-L1 expression when cases are stratified by TILs activation status, with higher PD-L1 expression in Group 3 compared to Group 1 and 2. No statistically significant difference of PD-L1 tumor expression by EGFR activation status.

Table 1:

Clinic-pathological characteristics of the NSCLC patients in Yale cohort A.

Yale Cohort A		
	n=299	(%)
Gender		
Female	152	50.8%
Male	147	49.2%
Age (years)	**(40–91)**	
<70	174	58.2%
≥70	125	41.8%
Stage		
0/IA	122	40.8%
IB	57	19.1%
IIA	32	10.7%
IIB	21	7%
IIIA	37	12.4%
IIIB	12	4%
IV	15	5%
Unknown	3	1%
Histology		
ADC	177	59.2%
SCC	62	20.7%
Other	53	17.7%
Unknown	7	2.4%
Smoking Statusx		
Non-smoker	34	11.4%
Smoker	255	85.3%
Unknown	10	3.3%